Techniques for generating attenuation map using cardiac SPECT emission data only: a systematic review

4 authors, including:

Getu Tadesse
Tehran University of Medical Sciences
1 PUBLICATION   **0** CITATIONS

SEE PROFILE

Parham Geramifar
Tehran University of Medical Sciences
66 PUBLICATIONS   **172** CITATIONS

SEE PROFILE

Eyachew Misganew Tegaw
Tehran University of Medical Sciences
1 PUBLICATION   **0** CITATIONS

SEE PROFILE

Some of the authors of this publication are also working on these related projects:

Project   Image Quality Improvement in Nuclear Tomographic Imaging (PET and SPECT) by using Machine/Deep Learning View project

Project   A New Approach for Attenuation Correction of Cardiac SPECT Data Using Emission Information in Dedicated ProSPECT Cardiac Scanner View project

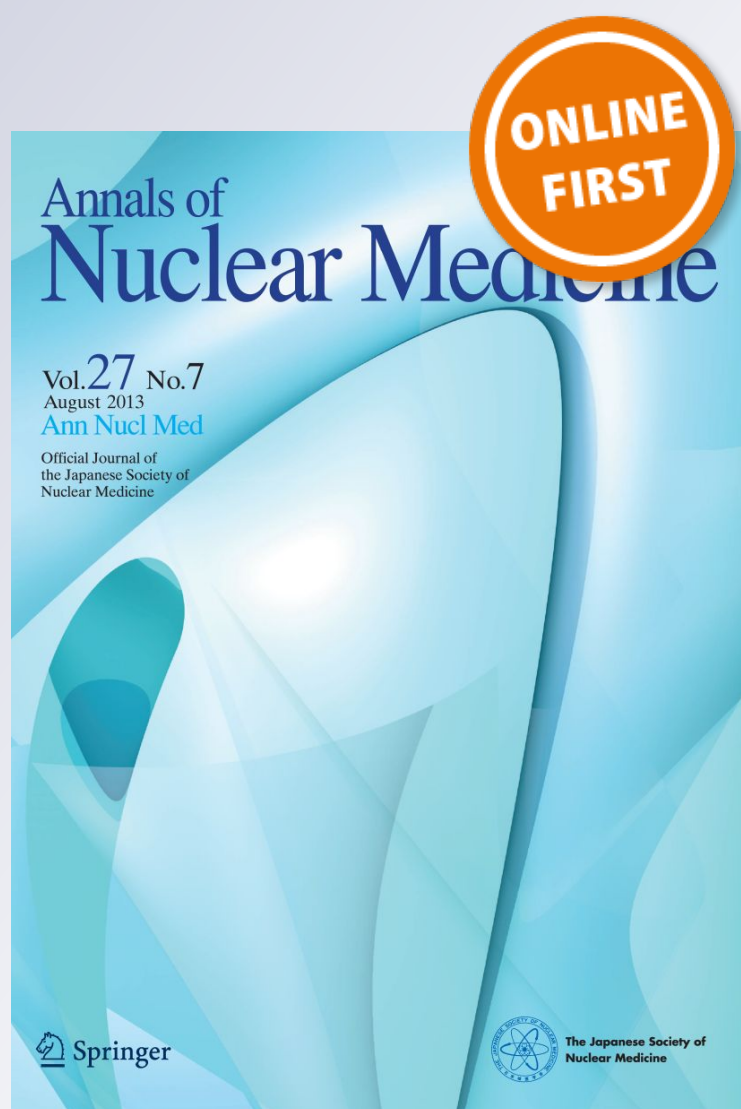# Techniques for generating attenuation map using cardiac SPECT emission data only: a systematic review

Getu Ferenji Tadesse, Parham Geramifar, Eyachew Misganew Tegaw & Mohammad Reza Ay

Annals of
Nuclear Medicine

Vol.27 No.7
August 2013
Ann Nucl Med

Official Journal of
the Japanese Society of
Nuclear Medicine

ONLINE FIRST

Springer

The Japanese Society of
Nuclear Medicine

Springer

Springer

CrossMark

Techniques for generating attenuation map using cardiac SPECT emission data only: a systematic review

Getu Ferenji Tadesse[1,2,3] · Parham Geramifar[4] · Eyachew Misganew Tegaw[1,2,5] · Mohammad Reza Ay[1,6]

Abstract

To reliably interpret and perform quantitative analysis, attenuation correction for cardiac single-photon emission computed tomography (SPECT) is fundamental. Thus, knowledge of the patient-specific attenuation map for accurate correction is required in SPECT quantitative imaging. The aim of this systematic review is to present general principles of attenuation correction and provide a structured summary of the approaches that have been proposed for generating the attenuation map for cardiac SPECT. We identified relevant articles published in English pertaining to the attenuation map (AM) determination using SPECT emission data only by searching PubMed, EMBASE, Scopus, and Web of Science databases. Moreover, other articles were hand searched. The protocol of this systematic review was registered in PROSPERO and the code given is CRD42017060512. Transmissionless techniques of determining attenuation map including calculated methods, statistical modeling for simultaneous estimation of attenuation and emission, consistency conditions criteria, using scattered data and other methods were reviewed. Methods for performing attenuation map for cardiac SPECT are developing and the progresses made are promising. However, much work is needed to assess the efficacy of the correction schemes in the clinical routine.

✉ Mohammad Reza Ay
mohammadreza_ay@tums.ac.ir

Getu Ferenji Tadesse
ofjan2007@gmail.com

Parham Geramifar
pgeramifar@tums.ac.ir

Eyachew Misganew Tegaw
eyachew1@yahoo.com

1   Department of Medical Physics and Biomedical engineering, School of Medicine, Tehran University of Medical Sciences, Tehran, Iran

2   Department of Medical Physics and Biomedical engineering, School of Medicine, Tehran University of Medical Sciences, International campus, Tehran, Iran

3   Department of Physics, College of Natural Sciences, Aksum University, Axum, Ethiopia

4   Research Center for Nuclear Medicine, Shariati Hospital, Tehran University of Medical Sciences, Tehran, Iran

5   Department of Physics, College of Natural Sciences, Debre Tabor University, Debre Tabor, Ethiopia

6   Research Center for Molecular and Cellular Imaging, Tehran University of Medical Sciences, Tehran, Iran

Introduction

Nuclear medicine is one of the most widely used non-invasive techniques for the assessment of coronary artery disease and other cardiovascular conditions. Single-photon emission computed tomography (SPECT) is a radionuclide imaging technique based on the principle of injecting a small quantity of a radiopharmaceutics into the body to monitor patient's physiologic function [1]. In a clinical routine, the physiologic function of human body is assessed by interpreting visually the result of radionuclide images. Myocardial perfusion imaging (MPI) using SPECT is a well-established non-invasive diagnostic method in the evaluation and risk stratification of coronary artery disease (CAD) [2]. Therefore, the improvement of dedicated cardiac SPECT directed to enhanced assessments of myocardial perfusion, precise measurements of ventricular motion, ejection fraction, and ventricular volumes was made possible using electrocardiographic gating [3]. However, several factors degrade the quality and diagnostic accuracy of emission tomography, including: attenuation of photons, scattered photons, the finite spatial resolution of the imaging system, the limited number of

Springer

counts, physiological as well as patient motion, and noise due to the random nature of the detection processes [4, 5]. Although these factors could limit the quantitative accuracy and quality of emission tomography, attenuation of photons is the most important factor that results in a lower diagnostic accuracy and lower specificity of detection of perfusion defects in MPI SPECT imaging [6, 7].

In quantitative cardiac SPECT, it is intended to provide a reconstructed image with one to one correspondence of the value of activity in each pixel with an area of patient's organ. Even though, it is not possible to eradicate completely the effects of soft-tissue attenuation which degrades quantifying SPECT images, minimizing those effects is important. To overcome this soft-tissue attenuation artifact: planar imaging (helpful in removing overlapping of inferior wall of heart with hemidiaphragm), supine plus prone imaging (used to overcome inferior wall attenuation artifact), ECG gating (helpful in distinguishing attenuation artifact from coronary disease) and image quantification were used [8, 9]. However, these indirect approaches were not able to overcome the problem of attenuation artifact which led to the developing of various algorithms to directly address the problem. Before any attenuation correction methods are applied for emission tomography image reconstruction, determination of an attenuation map which is the spatial distribution of linear attenuation coefficients is fundamental [10].

Generally, the methods for generating the attenuation map for SPECT can be categorized as either transmissionless or the transmission scanning which include an external radionuclide or X-ray computed tomography (CT). However, using transmission method to develop an attenuation map has the following limitation. CT-based attenuation correction (CTAC) systems result in increased radiation dose to the patient and the majority of systems used for cardiac imaging is SPECT standalone due to the fact SPECT/CT is expensive. Moreover, in some cases the nuclear medicine physicians believe that CTAC overestimate the activity. Using external radionuclide or line source has the limitation of increasing imaging time, and reducing the field of view (FOV), because they use a fan or cone beam, spillover, complicated data acquisition and processing, increase radiation to technologist and nonhomogeneous flux. Therefore, finding an easy, safety and low-cost solution for AC in SPECT is paramount.

Therefore, studies on attenuation correction methods which depend greatly on the accuracy of determining attenuation map using emission data only help to minimize the difficulties and attain the aim of a more accurate quantification. It is thus an opportune moment to systematically review the basic principles of attenuation correction and to synthesize the approaches that have been proposed for performing an attenuation map. This review presents the physical and methodological basis of attenuation correction and summarizes

the recent developments in algorithms used to compute the attenuation map in emission computed tomography (ECT).

Materials and methods

This systematic review was performed using a pre-specified protocol with the aim of reviewing the techniques that determine the attenuation map using cardiac SPECT emission data for appropriate attenuation correction. The statement of preferred reporting items for systematic reviews and meta-analyses (PRISMA) has been followed for reporting of this study [11].

Literature search

We identified relevant articles published in English pertaining to the methods of attenuation map determination in SPECT imaging using emission data only. The databases searched were PubMed, EMBASE, Scopus, and Web of Science. A core strategy was developed in PubMed and then translated for each database. All search strategies were developed using a combination of controlled vocabulary and keyword terms to define the concepts of attenuation correction and attenuation map in SPECT imaging. The following search algorithm was used for keywords: ((((((attenuation correction [tiab]) OR attenuation map [tiab])) AND ((((cardiac [tiab]) OR cardiac[MeSH Terms]) OR myocardial[tiab]) OR myocardial[MeSH Terms])) AND (((single photon emission tomography[tiab]) OR single photon emission computed tomography[MeSH Terms]) OR SPECT[tiab])) AND ((emission data[tiab]) OR scattered data[tiab])). A hand search was also done for additional relevant studies using references from retrieved articles. Conference abstracts and unpublished studies were excluded. The first searches were run on March 19, 2017 and the second searches were run again on March 17, 2018 to include recently published articles. However, there was no new article found which fit the selection criteria. The result of the first search was combined with the second search result and duplicates were removed. Then, the articles were downloaded to Endnote (version X7, for Windows operating system, Thomson Reuters, Philadelphia, PA, USA) to maintain and manage citation and facilitate the review process. All citations were imported into a reference management system and duplicates were removed.

Identification and selection of studies

Studies comprised any published articles that assessed determination of attenuation map of cardiac SPECT using emission data were retained. The included articles in our analysis had to meet the selection criteria given as follows: (a) evaluating attenuation correction of cardiac SPECT using

emission data; (b) generating attenuation map from emission data or scattered data; (c) when the data appeared in more than one article, the article with most details or recently published was considered.

Exclusion criteria

We excluded the articles based on the following criteria: (a) non-SPECT studies; (b) non-emission data (c) Reviews, case reports, conference proceedings and letters; (d) non-English studies; (e) studies that were conducted on transmission data; (f) repeatedly published literatures or similar literatures. Studies with different methods or algorithms for attenuation correction by generating attenuation map for cardiac SPECT using only emission data were all considered and were not excluded.

Selection of articles

Two independent reviewers (GFT and EMT) screened all articles returned by the search strategy by reading the title and abstract for their eligibility based on inclusion and exclusion criteria mentioned above. If the abstract is line with the subject at hand, a full-text assessment was done. Then, the full text of appropriate articles retrieved was retained and screening list was filled to select the final articles for review.

Result

Literature search

Search results are summarized in Fig. 1. In the initial search, we found 652 records in total, PubMed [20], Scopus [284], Web of Science [332] and Embase [16]. From the 652 records, 403 remained after removing duplication. By reading the title and abstract of each article, according to the inclusion and exclusion criteria, we excluded 298 articles and then 89 articles by reading the full text. Reasons for the exclusion of the other 89 articles were as follows: articles not reporting methods for generating attenuation map ($n=70$); besides those concerned transmission-based attenuation map determination using computed tomography (CT), and transmission line source ($n=19$). Finally, a total of 19 articles [1, 12–29] including 3 articles identified by hand search selection were used in this systematic review.

Methods for generating SPECT attenuation map

By now, the methods for generating the attenuation map for SPECT generally can be categorized as either transmission-less or the transmission scanning.

Transmission approach

For emission tomography, the spatial distribution of attenuation coefficient and its impact on the projection images is unknown and therefore additional information is needed to correct for these effects. These information can be generated utilizing an external radionuclide source [1, 8, 30–32]; or X-ray CT [7, 8, 10, 33–35], or segmented magnetic resonance images (MRI) [5]. However, except MRI segmentation technique, transmission-based attenuation correction obviously increases the patient's dose.

The CT-based attenuation correction (CTAC) results in increased radiation dose, which is a cause of distress for the patients' health [36, 37], as a study conducted in the United States shows about 0.4% of all cancers may be caused by radiation from CT studies [38]; increased cost, metal-induced or beam-hardening artifact, and misregistration of emission and transmission scans [39, 40]. However, it has wide application in nuclear medicine imaging as it performs high-quality attenuation correction for the radiopharmaceutical distribution in addition to improved anatomic localization. Many institutions currently use this technique and produce a high-quality image of tissue attenuation coefficients representing body anatomy. To standardize the data and provide a sufficient gray scale for display, the data are typically converted to CT numbers (Hounsfield units), by normalizing to the attenuation coefficient of water using Eq. (1):

$$CT_{number} = 1000\left(\frac{\mu(x,y)}{\mu_{water}} - 1\right), \qquad (1)$$

where the CT numbers of air and water are -1000 and 0, respectively.

The CT data can then be used to correct for tissue attenuation in the SPECT scans on a slice-by-slice basis [41]. CT values cannot directly used to correct the emission data for photon attenuation. There are three methods for conversion of CT values to correct emission data: segmentation, scaling, and dual-energy CT scans [42].

Segmentation

This is the method of separating CT image into regions equivalent to different tissue types (e.g., soft tissue, lung, bone). The generated CT image values for each tissue type are then replaced with appropriate attenuation coefficients at the gamma ray energy of the radionuclide used in the SPECT acquisitions. However, the main problem for this method is, the densities of some tissue regions are not uniform that may not be correctly represented by a separate set of segmented values. In pulmonary regions, for example, the density of lung tissue varies by as much as 30% [42].
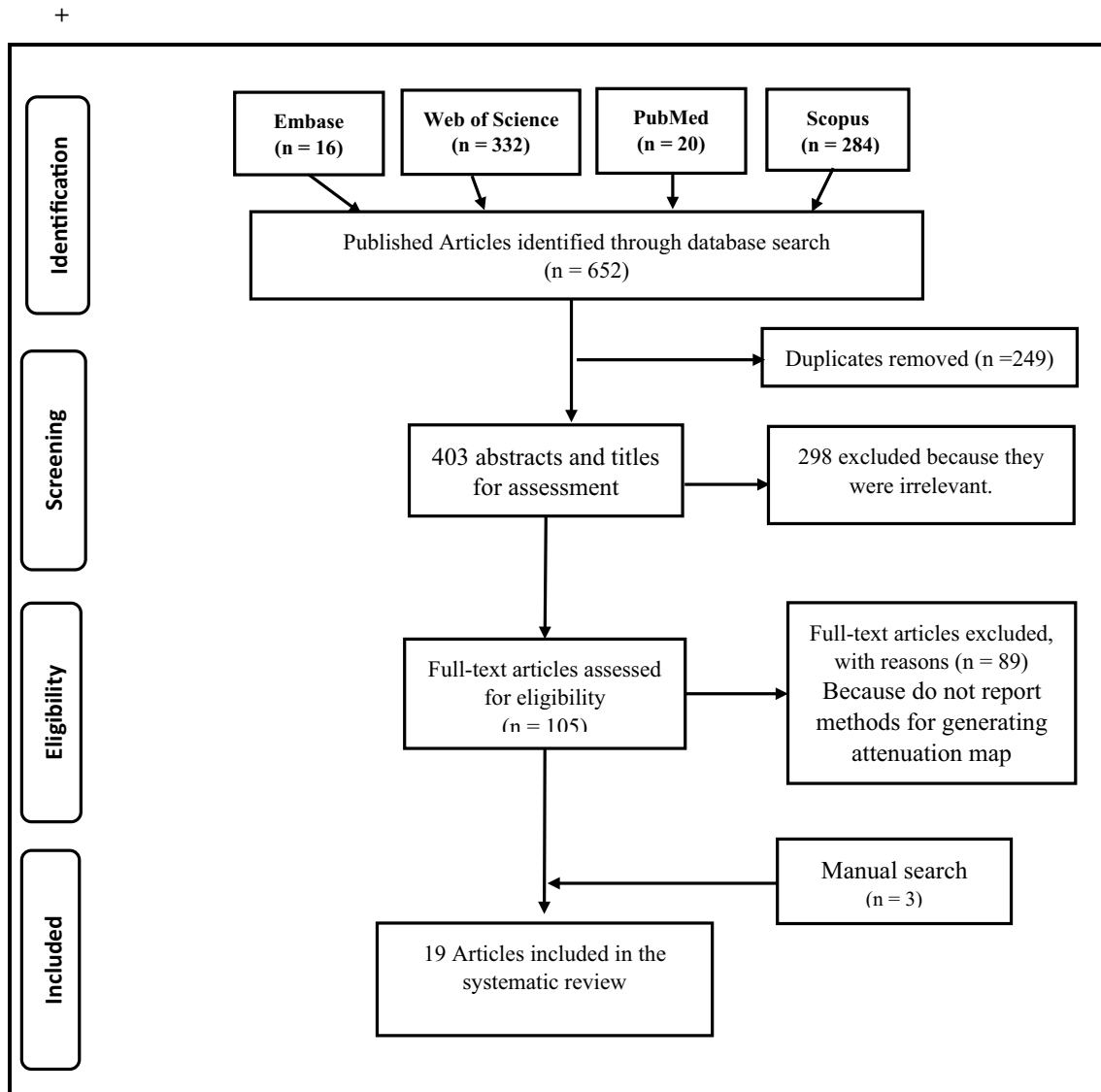
+

**Fig. 1** PRISMA flow diagram for the systematic review

Scaling

As the linear attenuation coefficient varies by photon energy, it is necessary to convert the attenuation data acquired with CT to match the energy of the radionuclide used in the SPECT acquisitions. This is done by applying a bilinear model relating attenuation coefficients at the desired energy to CT numbers measured at the effective energy of the CT beam of X-rays, as shown in Fig. 2. For CT values < 0, the measured tissue is expected to be a mixture of air and water, and the attenuation coefficient at the desired energy (e.g., 140 keV) can be calculated from the CT number by the following equation [41]:

$$\mu_{\text{tissue},140 \text{ keV}} = \frac{\text{CT\#} \times \left(\mu_{\text{water},140 \text{ keV}} - \mu_{\text{air},140 \text{ keV}}\right)}{1000}. \quad (2)$$

This equation describes the first component of the bilinear curve in Fig. 2 which is the linear scaling that leads to proper attenuation coefficients for low-Z materials [42]. For CT values > 0, the conversion became more difficult because the measured tissue is a combination of water and bone. In this case, the attenuation coefficient at the desired energy (e.g., 140 keV) can be calculated from the CT number by the following equation [41]:

$$\mu_{\text{tissue},140 \text{ keV}} = \mu_{\text{water},140 \text{ keV}}$$
$$+ \frac{\text{CT\#} \times \mu_{\text{water},\text{keVof}f} \times \left(\mu_{\text{bone},140 \text{ keV}} \times -\mu_{\text{water},140 \text{ keV}}\right)}{1000 \times \left(\mu_{\text{bone},\text{keVoff}} - \mu_{\text{water},\text{keVoff}}\right)}. \quad (3)$$

This equation describes the second component of the bilinear curve in Fig. 2.
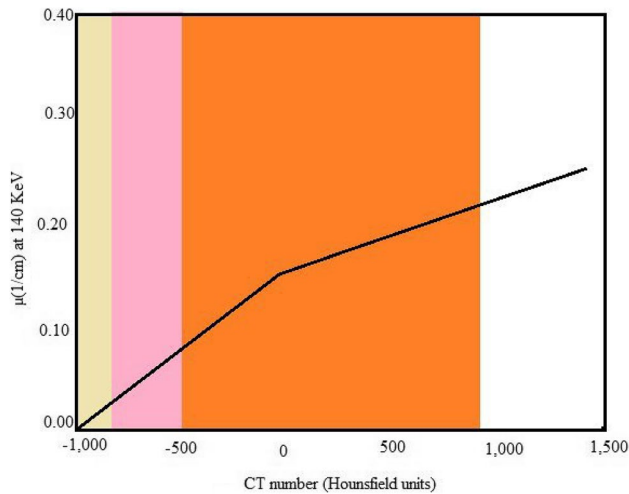
Fig. 2 Bilinear model commonly used for converting measured CT numbers to attenuation coefficients for specific radionuclide such as Tc-99m (140 keV gamma energy) [41]

Hybrid method

It is an alternative approach for converting CT images to attenuation map which combines segmentation and scaling [43]. The attenuation map is generated by first using a threshold to separate out the bone component of the CT image, and then separate scaling factors used for the mass attenuation coefficients of the bone and non-bone components. The threshold for differentiating bone from non-bone regions was selected to be 300 HU, based on heuristic arguments which are in contrast with the bilinear scaling method. Bilinear method can be considered as combining an air/water mixture model for $-1000 < H < 0$ and a water/bone mixture model for $H > 0$, the hybrid method can also be considered as an air/water mixture model for $-1000 < H < 300$ and an air/bone mixture model for $H > 300$. This can be seen by extrapolating the $H > 300$ segment to $H = 0$ [42].

Although hybrid SPECT/CT provides an accurate attenuation correction, this system can be used only to produce an attenuation map for radionuclides emitting gamma rays of a single energy (e.g., ^{99m}Tc at 140 keV). Therefore, this technique must be modified to calculate an attenuation map for dual energy windows (e.g., Tl-201 and In-111). Seo et al. [44, 45] has reported the way of calculating attenuation map for dual energy-emitting radionuclides in which the effective attenuation coefficient for photons of two different energies from a single radionuclide is expressed by Eq. (4):

$$\mu_{\text{eff}} = \frac{\ln\left(\exp[-\mu_1 x] + \alpha \exp[-\mu_2 x]\right) - \ln(1 + \alpha)}{-x}, \quad (4)$$

where μ_1 and μ_2 are attenuation coefficients for each gamma energy, α is the ratio of the branching ratios, and x

is the thickness of the medium through which the gamma rays pass. μ_1 and μ_2 can be obtained from tabulated values [46] with α calculated from the branching ratios (i.e., 94, 90.2%) of the 171 and 245 keV gamma rays (i.e., $\alpha = 94\%/90.2\% = 1.042$) for In-111 and for Tl-201, α calculated from branching ratios (i.e., 90.22, 9.78%) of the 70 keV X-ray and 167 keV gamma ray (i.e., $\alpha = 90.22\% / 9.78\% = 9.22$).

It has been reported that, myocardial images of dual energy window using low-energy high resolution (LEHR) collimator has the utility for adding myocardial counts and improving inferior attenuation artifact [47, 48]. Therefore, dual energy images of Tl-201 myocardial SPECT have several advantages in clinical routine.

Drawbacks of using an external radionuclide source for generating attenuation map are described as follows: increases the time required to treat a patient, contamination of emission photons with transmission photons and misregistration between the transmission dataset with the emission dataset. Moreover, patients may not tolerate longer scan time if multiple imaging sessions are needed, and this leads to the registration problem in emission image reconstruction [49].

Transmissionless approach

Researchers are attempting to generate an attenuation coefficient map without adding a separate transmission scan from the emission data to avoid the difficulties of transmission acquisition. Algorithms presented in this review methods either assume a uniform distribution of attenuation coefficients assigned to segmented body area or determining attenuation map directly from emission data. The idea of using transmissionless method to generate attenuation map for the attenuation correction in SPECT has had a long history, starting with the innovative work of Censor et al. [14]. The techniques that have been proposed to date can be divided in to: calculated methods [1]; simultaneous reconstruction [14, 16, 19, 23, 26]; consistency conditions criteria [12, 15, 21, 25, 28, 29]; techniques using scattered data [13, 17, 20, 24, 27] and other methods [22, 50, 51].

Calculated methods

In the region with uniform attenuation such as brain and abdominal area, the body outline can be determined from emission data, then the spatial distribution of linear attenuation coefficient value can be assigned to the defined region based on the type of tissue to create the corresponding attenuation map [1]. The body outline can be determined either manually, or automatically using edge detections methods. However, determination of patient contour from emission data alone without the use of any transmission data is not an easy task.

Methods based on consistency conditions

Another method for obtaining the attenuation maps for cardiac SPECT was the direct approximation from the emission data, without transmission imaging, based on consistency conditions of the attenuated Radon transform. The first consistency method to estimate attenuation distribution from emission data assumes that the true attenuation distribution is approximately an affine distortion of a known prototype attenuation distribution as proposed by Natterer [21] in 1993. In this study, a uniform circle with a given constant attenuation coefficient was used. As the attenuation map is a distortion of the initial uniform attenuation map, the modified projection will only depend on the values of the affine transformation. This method has been shown to work using simulated images, but it is not accurate when applied to emission data acquired by a gamma camera, due to the geometric response of the collimator and the scatter.

The two-dimensional attenuated radon transform should satisfy a set of consistency conditions, derived from the Helgason–Ludwig conditions described by the Eq. (5): [15, 16, 21, 28, 29].

$$\int_{0}^{2\pi} e^{ik\phi} \int_{-\infty}^{\infty} S^m e^{\frac{1}{2}(T(\theta,s)+iHT(\theta,s))} g(s,\theta) \mathrm{d}s \mathrm{d}\phi = 0, \tag{5}$$

where s is the detector bin; θ is the angle projection where $\theta = (\cos\varphi, \sin\varphi)^{\mathrm{T}}$; m is the moment order and k is an integer, with $0 \le m < k$; $g(\theta, s)$ represents the measured data or emission sinogram (attenuated Radon transform of activity distribution); $T(\theta, s)$ represents the transmission sinogram (non-attenuated Radon transform of the attenuation distribution); H represents the Hilbert transform operator that acts on $T(\theta, s)$ as a function of s.. If $g(\theta, s)$ is supplied by the measured emission data of a SPECT system, then the consistency conditions become a set of nonlinear equations for the unknown transmission data $T(\theta, s)$. Using iterative reconstruction algorithm transmission data $T(\theta, s)$ can be reconstructed to obtain the attenuation distribution. Because of the association of transmission sinogram with the emission sinogram in consistency conditions, they have become tremendously useful in the case of SPECT where an attenuated radon transform estimated the measured data.

Welch et al. [28] used the consistency conditions to define the transmission data in SPECT as consistency transmission SPECT (ConTraSPECT) to find the uniform elliptical attenuation object which was consistent with the SPECT projection data. During the reconstruction of emission data, in fact, this object is used for attenuation correction. Some of the physical factors which degrades the SPECT data are geometric: the response of the collimator and Compton scatter. Welch et al. succeeded to estimate the boundary of a uniform attenuation distribution by simulating the effect of collimator geometric response and scatter with simulated Monte Carlo method and experimentally acquired projection data. The method was tested using both experimental and simulation studies. The results of the experimental study show that ConTraSPECT method can be used to estimate the attenuation distribution from real cardiac SPECT data for attenuation correction. However, the consistency conditions were not sufficient to accurately optimize an attenuation map where both the organ contours and attenuation are unknown and reconstructions were not converging to an acceptable solution [52].

Bronnikov et al. [12] has attempted to apply discrete consistency conditions which strengthen the model of the consistency conditions, using a matrix representation in place of the continuous transform. This approach is helpful to determine the attenuation map without reconstructing the activity distribution by solving the problem reduced to a set of nonlinear algebraic equation. Such an approach confirms a natural regularization of the problem, letting one to use the well-known method of Tikhonov regularization. The algorithm was also tested using real data acquired of a physical torso phantom. The resulting reconstruction proven to be acceptable corresponding to the spine was incorrectly located in the reconstruction, appearing significantly closer to the center of the body than in the true phantom. Moreover, the main advantage of this method over the continuous description is that it can easily be applied in various scanning configurations. This method takes into account the influence of various physical factors, such as finite detector resolution, system response, and scatter, which may considerably improve the accuracy of the modeling and can avoid crosstalk between the attenuation map and the source distribution.

Another approach for obtaining the non-uniform attenuation map with regions of different attenuation from the emission data using the data consistency conditions of the attenuated Radon transform was proposed by Yan and Zeng [29]. The method was based on deriving boundaries of the constant regions of the true attenuation map using an iterative algorithm. Using the exist crosstalk effects between attenuation map and activity images, the boundaries of the constant regions of the attenuation map were then derived and automatic segmentation can be performed for regions with sharp boundaries. The crosstalk effects are as a result of the negative attenuation map which is superimposed on the activity reconstruction, and the negative activity distribution which is superimposed on the attenuation map reconstruction. The crosstalk effects are illustrated in Fig. 3 [29].

Finally, by assigning a constant linear attenuation coefficient in each segmented region, the attenuation map for cardiac SPECT data can be obtained. The method was tested using the Monte Carlo simulated data for a non-uniform
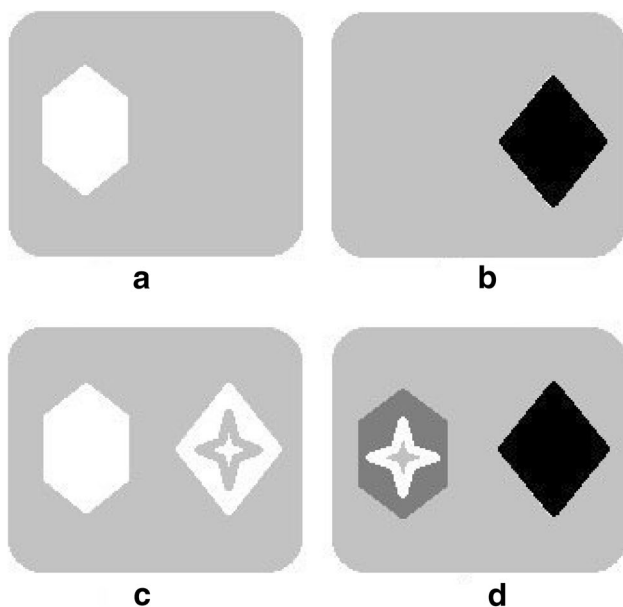
Fig. 3 Crosstalk effects: **a** the original activity image, **b** the original attenuation map, **c** the reconstructed activity image, the region marked by star comes from the attenuation map due to the crosstalk. **d** The reconstructed attenuation map, the region marked by star comes from the activity due to the crosstalk [29]

attenuation map. The resulting simulation has been shown to work effectively for non-uniform attenuators providing the exact boundaries of the constant regions of the attenuation map; however, the algorithm failed in high noisy and blurry images.

Simultaneous reconstruction

Recent methods aim to simultaneously reconstruct correction factors for both estimated activity and attenuation. This can be obtained by solving the nonlinear equation relating to the attenuation map and activity distribution using an iterative technique. This approach was first proposed by Censor et al. [14] in the late 1970s in which alternating iterations of the reconstruction algorithm was used to reconstruct emission tomograms and attenuation maps from a set of emission projections alone which has been explored after then by many studies [14, 16, 19, 23, 26].

Nutys et al. [23] formulated a maximum-likelihood reconstruction of attenuation and activity (MLAA) method for SPECT and positron emission tomography (PET) incorporating some prior knowledge to compute attenuation map directly from the emission sinogram without transmission scan. The prior knowledge incorporated into the algorithm are the probability distribution of attenuation coefficients and Gibbs distribution to encourage local smoothness. The algorithm was tested using simulations and clinical studies. Good results were obtained in the case of uniform

attenuation in attenuating body and a good agreement was shown between MLAA reconstruction and the image obtained with attenuation correction from a transmission scan.

Krol et al. [19] have developed the techniques of joint estimation of the attenuation and activity from SPECT emission sinograms using maximum-likelihood optimization. Since the algorithm used activities within the patient (intrinsically) as transmission sources to estimate attenuation coefficients, it is called expectation maximization intrinsic transmission SPECT (EMIS). Similar to Nuyts's algorithm, it is based on a Poisson noise model for the projection data. In the case of determining the linear attenuation coefficients, they applied two methods: the attenuation parameters were estimated with the emission intensities fixed at their true value. The result was an accurate reconstruction of attenuation. The second method was simultaneous estimation of activity and attenuation parameters from the emission data alone. To evaluate this technique, simulation and physical phantom studies were performed. The result of the study have shown that there was crosstalk between estimates of activity and attenuation distribution which limits the ability of the algorithm to distinguish higher attenuation combined with higher activity from lower attenuation combined with lower activity. Furthermore, the result of comparison of EMIS with conventional MLEM assuming a fix attenuation map has shown that EMIS demonstrates less contrast between soft tissue and heart, lungs, and spine. However, EMIS approximations of activity and attenuation distribution in the heart, spine, lungs and soft tissue were well-outlined and correctly located [53, 54].

Gourion et al. [16] proposed an approach in which simultaneous estimation of the unknown attenuation coefficient and the emission source using only the emission data was performed based on nonlinear optimization techniques. Similar crosstalk effects are seen in a regularized nonlinear optimization technique. The method was evaluated using simulation in which several optimization strategies have been compared and phantom experiment. The phantom experimental result has shown that relative quantitative attenuation correction was improved over the ConTraSPECT and the contour method.

The main challenge of estimating simultaneous attenuation parameters and emission parameters was the image artifact caused by crosstalk between the estimated attenuation and activity distribution. To reduce the extent of the problem, Salomon et al. [26] formulated the simultaneous reconstruction method to effectively avoid these crosstalk artifacts using a priori knowledge from anatomical atlas information. A 3D organ is coarsely registered to the SPECT data via anatomical landmark detection. Based on the patient history, each organ structure is then identified with its typical attenuation coefficient to develop an initial estimate for the

attenuation map. The performance analysis of the algorithm was done by simulation and patient SPECT data. The results demonstrated have shown that there was a good agreement of attenuation map derived from the algorithm with the data generated from the transmission scan.

Scattered data method

There are other algorithms that use scattered data to reconstruct the attenuation map since attenuation is a direct consequence of Compton scattering. If the attenuation parameters can be obtained from scattered data, the additional transmission scan instrument for the attenuation correction may not be required. To determine a segmented attenuation map, scattered data is used to highlight the boundaries between different tissues and the predefined attenuation coefficients are assigned to the segmented region. Jha et al. [17] investigated the possibility of joint reconstruction of the activity and attenuation map using list mode (LM) SPECT data, including the scattered-photon data. List mode refers to a special scanning mode in which each event and its precise time of occurrence is recorded sequentially. A path-based formalism to study the information content of LM scattered-photon data was proposed. As photoelectric and Compton scatterings are the main photon interaction mechanisms within the tissue of SPECT imaging energies, it is expected that the scattered-photon data should provide information about the attenuation map of the tissue. Moreover, acquiring data using LM format has its own advantage over the convectional detection systems by avoiding the loss of information due to the binning process.

Sitek et al. [27] have developed an approach which utilizes image information recorded in several scatter windows below the principal photopeak window, assuming that all photons were only scattered once. They have shown the linearity between detected counts in the scatter windows and voxel attenuation coefficients. The probability of the number of photons detected in each scatter window and the voxel attenuation coefficient were modeled using statistical techniques and prior knowledge of Compton scattering angles with respect to its energy. The algorithm was tested by acquiring projection datasets of a torso phantom using a Siemens SPECT scanner. The result was good for torso phantom; however, the regions of the lungs were not well-defined in the boundaries.

Cade et al. [13] developed the scatter model to estimate attenuation map from the scattered photons. For estimation of both attenuation coefficient map and activity distribution, they have been developed an iterative algorithm with the maximum-likelihood expectation maximization algorithm to iteratively update attenuation map for attenuation correction and source distribution based on the scatter photon. The algorithm was tested using simulated data showing good results with photons limited to single scattering event. The reconstruction has been further improved when both algorithms, scatter-based maximum-likelihood gradient ascent (SMLGA) algorithm and MLAA algorithm were combined.

Pan et al. [24] estimated the regions of the lungs and non-pulmonary tissues of the chest by segmenting the photopeak and Compton scatter window images to identify the outline of the lung and soft tissues and then assigning predefined attenuation coefficients to the segmented lung and soft-tissue regions. This approach was assessed by both phantom and patient studies, and comparison was made using transmission imaging with a slant-hole collimator. Despite some errors in the estimate of the lung volume, the resulting segmentation provided good agreement and acceptable accuracy in the reconstruction of the body outline and lung regions using only emission images of the phantom and patient data. In both studies, attenuation correction using MLEM was performed and uniformity within the heart walls was observed over the images without attenuation correction and scatter correction.

Likewise, Maeda et al. [20] also developed a new technique to generate a non-uniform attenuation coefficient which is called segmentation of scatter and photopeak window data for attenuation correction (SSPAC). SSPAC method requires the following main ideas for developing attenuation map. First, segmenting body lines and lung contours using reconstructed scatter image. Second, segmenting myocardium and liver using photopeak image. Third, obtaining average models of the mediastinum and thoracic spine by X-ray computed tomography. Fourth, generating attenuation coefficient map and assigning attenuation values for bone, soft tissue, and lung. Finally, applying a Gaussian filter to the Attenuation map for the system resolution compensation. The processes for constructing segmentation with of SSPAC and non-correction images are shown in Fig. 4 [55].

The clinical feasibility of SSPAC for the detection of coronary artery disease [55] and in normal subjects [56] were evaluated and the sensitivity, specificity, and accuracy of this new correction method with that of conventional non-attenuation corrected myocardial perfusion were compared. The results demonstrated that the SSPAC improved detection ability in the left anterior ascending (LAD) and right coronary artery (RCA) territories, significantly higher sensitivity and negative predictive value (NPV) in the LAD territory as well as significantly higher specificity, accuracy, and positive predictive value (PPV) in the RCA territory. Currently, the application of this technique has been commercially available from Canon Medical Systems (Tokyo, Japan) for clinical routine.
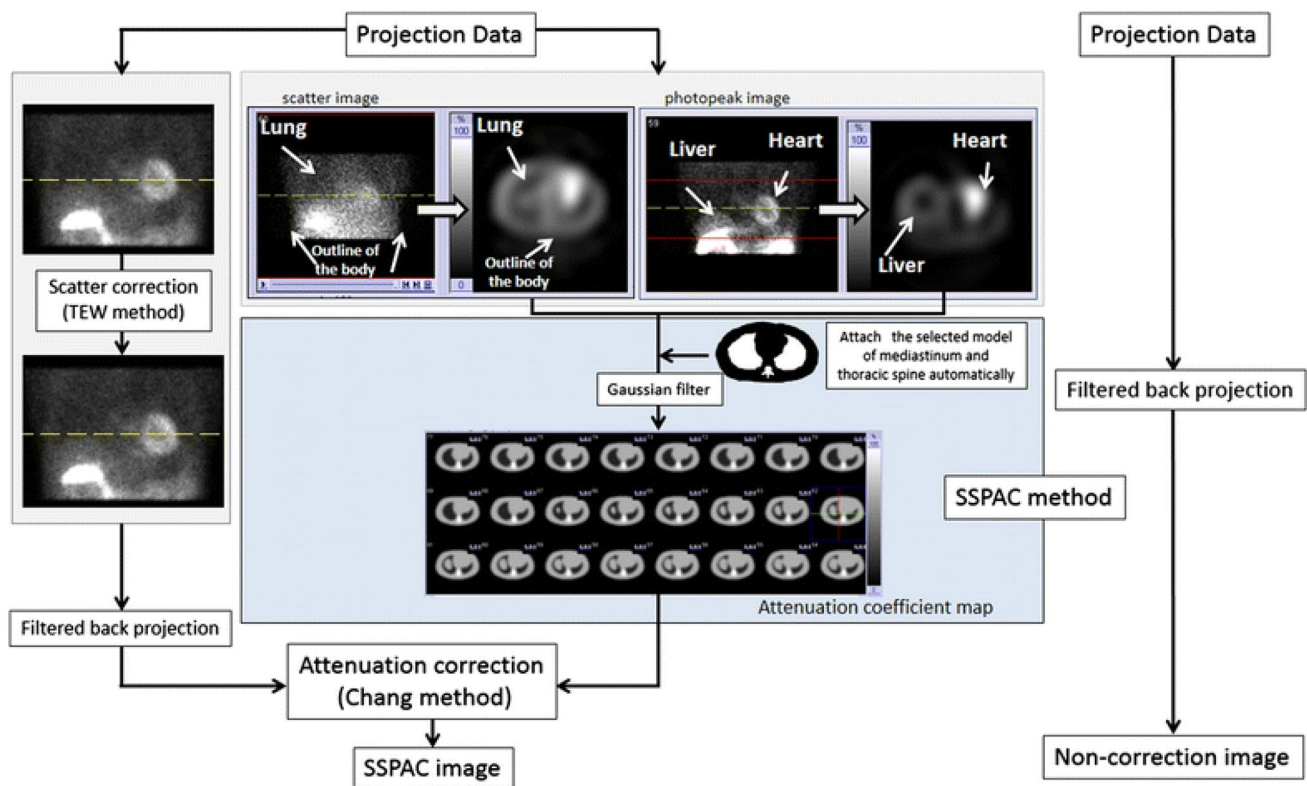
Fig. 4 The processes for constructing segmentation with scatter and photopeak window data for attenuation correction (SSPAC) images and non-correction images [58]. *TEW* triple-energy window

Others methods

Another approach, which did not receive considerable attention, was formulated by Noumeir and El-Daccache [22]. They determined the boundary of the uniform attenuation map by detecting the surface of the patient body from the emission data. To minimize the image noise and define the body outline correctly, they have developed the 3D generalization active counter model known as snakes. The algorithm was applied to reconstructed emission volume to determine the outline of the heart for attenuation correction. Moreover, uniform attenuation was corrected using body segmentation obtained by the active counter and non-uniform attenuation was corrected using transmission attenuation map, where the difference revealed was insignificant.

Kaplan et al. [50] have developed a method to determine attenuation from differential attenuation information (DAI) in which SPECT emission data were produced from multiple energy emission isotopes. It was shown that the attenuation along each projection line is proportional to the difference in attenuation for two emissions at separate energies. The feasibility of attenuation compensation using DAI was investigated using synthesized scatter-free data from an anthropomorphic digital phantom. The results show an improved accuracy of the reconstructed images when using DAI as compared to non-attenuation correction or using a uniform attenuation correction. However, it has not been tested with data including scatter which would have a significant effect on the accuracy of the reconstruction.

Madsen et al. [52] proposed a method to generate attenuation map based on determining boundaries of the lung and the subject's body contour and assigning appropriate attenuation coefficient for the photon energy used in the study. To overcome the problem of determining the lung region accurately from emission photons, because of the low density of the lungs which creates nonhomogeneous tissue attenuation, they have administrated a small amount of ^{99m}Tc macroaggregated albumin (MAA). However, this method requires the injection of an additional radiopharmaceutical agent, which may interfere with imaging of the perfusion agent and gives more exposure to the patient.

Discussion

Systematic reviews of literature show that many of the researchers have attempted to determine an attenuation map for SPECT imaging using emission data only. They mainly focused on solving the impact of soft-tissue attenuation on apparent tracer distribution, because of the fact that

Table 1 Summary of determination of attenuation map methods using emission data only

Class of transmissionless methods	Authors	Publication year	Ways of generating attenuation map
Calculated methods	Zaidi and Hasegawa [1]	2003	In the region of uniform attenuation such as brain and abdominal area, the body contour can be determined from emission data, then the region within the counter can be assigned a uniform linear attenuation coefficient value. Body counter can be determined either manually or with automatic edge detections methods
Consistency condition	Natterer [21]	1993	A method for computing the attenuation distribution from the emission data by assuming that the true attenuation distribution is approximately an affine distortion of a known prototype attenuation distribution is described
	Bronnikov [12]	2000	The discrete consistency conditions provide a relatively simple algorithm, whose stability can be controlled by the well-established method of Tikhonov regularization was shown
	Welch et al. [28]	1997	Consistency conditions were used to find the uniform elliptical attenuation object which is most consistent with the measured emission data. The method consists of finding the uniform elliptical attenuation distribution most consistent with SPECT data
	Gourion et al. [16]	2002	An approach which simultaneously estimates the unknown attenuation coefficient and the emission source using the emission data only were considered. A regularization approach based on nonlinear optimization techniques was used. Two programs P and G, based on a Poisson and a Gaussian likelihood function are compared and their viability is substantiated using a simulated case study and a phantom experiment
	Yan and Zeng [29]	2009	A new method to estimate the attenuation map using the data consistency conditions of the attenuated Radon transform which based on deriving boundaries of the constant regions of the true attenuation map using an iterative algorithm was proposed. This new method is tested by Monte Carlo simulations with the attenuation and scattering effects
	Panin et al. [25]	2001	An iterative algorithm that reconstructs the attenuation map and emission activity distribution from SPECT emission data is proposed. The algorithm is based on the quasi-linearized attenuated Radon transform. They proposed obtaining the attenuation map based on a ''knowledge set'' and the unknowns were the coefficients of the principle components in a singular value decomposition
Simultaneous reconstruction	Censor et al. [14]	1979	Alternating iterations of the reconstruction algorithm were used to reconstruct emission tomograms and attenuation maps from a set of emission projections alone
	Nuyts et al. [23]	1999	A new maximum-likelihood method was derived for simultaneous reconstruction of the activity distribution and attenuation map in PET and SPECT and the performance of the algorithm was evaluated using simulations and clinical studies
	Salomon et al. [26]	2009	With the simultaneous reconstruction method presented, effectively preventing the typical cross-talk artifacts using a priori known atlas information of a human body was proposed
	Krol et al. [19]	2001	EM algorithm to optimize the likelihood for simultaneous reconstruction of attenuation and activity from SPECT emission sinograms was derived
	Gourion et al. [16]	2002	A regularization approach based on nonlinear optimization techniques was used. Two programs P and G, based on a Poisson and a Gaussian possibility function are compared and their viability is substantiated using a simulated case study and a phantom experiment

Table 1 (continued)

Class of transmissionless methods	Authors	Publication year	Ways of generating attenuation map
Using scattered data	Jha et al. [17]	2013	Joint reconstruction of the activity and attenuation map using list mode (LM) SPECT emission data, including the scattered-photon data was investigated
	Pan et al. [24]	1993	Estimation of patient-specific attenuation maps using the photopeak and scatter window slices from 16 consecutive 99mTc-labeled sestamibi perfusion studies were segmented interactively
	Sitek et al. [27]	2007	An approach which utilizes image information recorded in several scatter windows below the principal photopeak window to estimate an additional set of projections whose values are linearly related to line integrals of attenuation coefficients across the object was developed
	Cade et al. [13]	2010	A scatter model to estimate attenuation map from scattered photon
	Maeda et al. [20]	2002	A new technique to generate a non-uniform attenuation coefficient which is called segmentation of scatter and photo peak window data for attenuation correction (SSPAC)
Others methods	Noumeir and El-Daccache [22]	1998	An approach which determines the boundary of the uniform attenuation map by detecting the surface of the patient body from the emission data was formulated. An active surface model which is a three-dimensional generalization of the active contour model known as snakes was used
	Kaplan et al. [50]	1999	A method to estimate attenuation from differential attenuation information (DAI) contained solely in SPECT emission data produced by ^{201}T1 or other multiple emission isotopes was proposed
	Madsen et al. [52]	1993	A method to generate attenuation map based on determining boundaries of the lung using small amount of 99mTc macroaggregated albumin (MAA) and the subject's body contour and assigning appropriate attenuation coefficient for the photon energy

soft-tissue attenuation reduces SPECT image quality, which in turn results in decreasing the possibility of detection of the lesion.

From the methods which have been developed to solve the problems of non-uniform attenuation transmission emission-based methods are clinically implemented. However, attenuation map which is generated from SPECT transmission projections is relentlessly incomplete because the transmission data cover only a part of the field of view. Moreover, the transmission data may contain high noise level and scatter which lead to severe artifacts in image reconstruction. Due to this fact, several studies have been conducted for attenuation correction without transmission measurements using only emission data (see Table 1). Calculated methods, statistical modeling for simultaneous estimation of attenuation and emission, consistency conditions criteria, using scattered data and other methods such as differential attenuation map technique, and patient body surface detection are among the methods proposed by the researchers in the field.

Each method has own advantages and limitations. For calculation method which was applied for the uniform attenuation areas such as brain and abdominal areas where soft tissues are the dominant constituent, a uniform linear attenuation value is applied to the corresponding region. However, this method is not effective for heterogeneous regions, such as the thorax. Because it is generally difficult to define the patient contour from emission data alone without the use of transmission data. Therefore, transmissionless techniques have had a limited clinical application.

The consistency conditions are helpful in the case of SPECT where the measured data approximate an attenuated Radon transform since they link the transmission sinogram with the emission sinogram. Therefore, the consistency conditions only contain one unknown quantity (the transmission sinogram) as opposed to the imaging equations where both the emission and attenuation distributions are unknown. Natterer [57] was able to derive the so-called consistency conditions, to provide a mathematical framework that verify a given estimate for the underlying attenuation and activity distribution with some limitations to identify a perfect match for 360° scan trajectories. The drawback of this method is that they are inefficient computationally and, moreover, most of these methods demand some additional knowledge of the problem to linearize and to stabilize it which needs

further improvement [12]. The consistency conditions can hardly prove useful for attenuation compensation with non-uniform attenuators and this limits clinical applications of these methods for cardiac imaging.

Another approach, receiving considerable attention is to compute the attenuation map directly from the emission data and eliminating the transmission scan from the acquisition protocol in a simultaneous reconstruction algorithm. The major limitation of most simultaneous methods is the inherent cross-dependency between activity and attenuation distribution, leading to noticeable artifacts. Compared to other simultaneous reconstruction approaches, the inclusion of a priori information such as typical attenuation coefficients and predefined anatomic structures inherently avoids typical cross-talk effects between the estimated activity and attenuation distribution [58].

Currently, a promising method to provide an alternative to transmission-based attenuation maps for quantitative SPECT imaging is using scattered data to estimate attenuation coefficient distribution in a patient. The interesting thing is that does not need additional acquisition time. Scatter window which is used for scatter correction can be used for estimating attenuation map as well. However, the potential limitations on the accuracy of correction inherent in the method, due to the estimation of the regions and assignment of the attenuation coefficients, need to be determined further, and the method needs to be further automated before it can be considered for routine clinical use.

Conclusion

Attenuation correction improves physician interpretation and quantification with attenuated corrected cardiac SPECT images and increases the importance of photons arising from a source located in the deep area of the patient's body, as tremendously decreased by attenuation. Thus, accurate correction for non-uniform attenuation in cardiac SPECT requires data of the patient-specific attenuation map for quantitative imaging. Transmissionless techniques of determining attenuation map which used for attenuation correction were reviewed and presented in this paper. Methods for performing attenuation map for cardiac SPECT are developing rapidly and its progress is promising. However, more work is needed to assess the routine clinical efficacy of the correction schemes.

Limitations

There are some limitations in our systematic review. The number of relevant studies was limited, the literature search was confined to English publications and incomplete retrieval of researches done so far, such as works in other language or unpublished works.

References

1. Zaidi H, Hasegawa B. Determination of the attenuation map in emission tomography. J Nucl Med. 2003;44(2):291–315.
2. van Dijk JD, et al. Value of attenuation correction in stress-only myocardial perfusion imaging using CZT-SPECT. J Nucl Cardiol. 2017;24(2):395–401.
3. Dvorak RA, Brown RKJ, Corbett JR. Interpretation of SPECT/CT myocardial perfusion images: common artifacts and quality control techniques. Radiographics. 2011;31(7):2041–57.
4. Zaidi H. Recent developments and future trends in nuclear medicine instrumentation. Zeitschrift für Medizinische Physik. 2006;16(1):5–17.
5. Zaidi H, Montandon ML, Slosman DO. Magnetic resonance imaging-guided attenuation and scatter corrections in three-dimensional brain positron emission tomography. Med Phys. 2003;30(5):937–48.
6. Plachcińska A, et al. Diagnostic performance of myocardial perfusion single-photon emission computed tomography with attenuation correction. Kardiologia Polska. 2016;74(1):32–9.
7. Apostolopoulos DJ, Savvopoulos C. What is the benefit of CT-based attenuation correction in myocardial perfusion SPET? Hell J Nucl Med. 2016;19(2):89–92.
8. Bateman TM, Cullom SJ. Attenuation correction single-photon emission computed tomography myocardial perfusion imaging. Semin Nucl Med. 2005;35(1):37–51.
9. Stathaki M, et al., The benefits of prone SPECT myocardial perfusion imaging in reducing both artifact defects and patient radiation exposure. Arquivos brasileiros de cardiologia. 2015. **105**(4):345–352.
10. Ljungberg M, Pretorius PH. SPECT/CT: an update on technological developments and clinical applications. Br J Radiol. 2018. 91(1081):20160402.
11. Moher D, et al. Preferred reporting items for systematic reviews and meta-analyses: the PRISMA statement. PLoS Med. 2009;6(7):e1000097.
12. Bronnikov A. Approximate reconstruction of attenuation map in SPECT imaging. IEEE Trans Nucl Sci. 1995;42(5):1483–8.
13. Cade S, et al., Estimating an attenuation map from measured scatter for 180° cardiac SPECT. J Nucl Med, 2010. 51:1357
14. Censor Y, et al. A new approach to the emission computerized tomography problem: simultaneous calculation of attenuation and activity coefficients. IEEE Trans Nucl Sci. 1979;26(2):2775–9.
15. da Silva AMM, Robilotta CC, Ieee, Attenuation correction in cardiac spect using consistency conditions. In: 2006 3rd IEEE international symposium on biomedical imaging: macro to nano, vols 1–3. 2006. p 271.
16. Gourion D, et al. Attenuation correction using SPECT emission data only. IEEE transactions on nuclear science. 2002;49(5):2172–9.
17. Jha AK, et al. Joint reconstruction of activity and attenuation map using LM SPECT emission data. In: Nishikawa RM, Whiting BR,

Hoeschen C, editors. Medical imaging 2013: physics of medical imaging, vol 8668. Bellingham, Washington: International Society for Optics and Photonics; 2013.

18. Kaplan M, et al. Generating attenuation maps using differential attenuation data. In: Nuclear science symposium, 1996. conference record, 1996 IEEE. 1996. IEEE.

19. Krol A, et al. An EM algorithm for estimating SPECT emission and transmission parameters from emission data only. IEEE Trans Med Imaging. 2001;20(3):218–32.

20. Maeda H, et al. Attenuation correction for myocardial SPECT: segmentation with scatter and photopeak window data for attenuation correction (SSPAC) method. J Nucl Med. 2002;43(5):230P-230P.

21. Natterer F. Determination of tissue attenuation in emission tomography of optically dense media. Inverse Probl. 1993;9(6):731.

22. Noumeir R, El-Daccache R. Attenuation correction in spect using active surfaces. In: Nuclear Science Symposium, 1998. Conference record. 1998 IEEE. 1998. IEEE.

23. Nuyts J, et al. Simultaneous maximum a posteriori reconstruction of attenuation and activity distributions from emission sinograms. IEEE Trans Med Imaging. 1999;18(5):393–403.

24. Pan TS, et al. Estimation of attenuation maps from scatter and photopeak window single photon-emission computed tomographic images of technetium 99 m-labeled sestamibi. J Nucl Cardiol. 1997;4(1):42–51.

25. Panin VY, Zeng GL, Gullberg GT. A method of attenuation map and emission activity reconstruction from emission data. IEEE Trans Nucl Sci. 2001;48(1):131–8.

26. Salomon A, Goedicke A, Aach T. Advanced reconstruction of attenuation maps using SPECT emission data only. In: Hsieh J, editors. Medical imaging 2009: physics of medical imaging, vol 7258. Bellingham, Washington: International Society for Optics and Photonics; 2009.

27. Sitek A, Moore SC, Kijewski MF. Correction for photon attenuation without transmission measurements using Compton scatter information in SPECT. In: nuclear science symposium conference record, 2007. NSS'07. IEEE. 2007. IEEE.

28. Welch A, et al. Toward accurate attenuation correction in SPECT without transmission measurements. IEEE Trans Med Imaging. 1997;16(5):532–41.

29. Yan Y, Zeng GL. Attenuation map estimation with SPECT emission data only. Int J Imaging Syst Technol. 2009;19(3):271–6.

30. Bailey DL. Transmission scanning in emission tomography. Eur J Nucl Med. 1998;25(7):774–87.

31. Tung C-H, et al. Nonuniform attenuation correction using simultaneous transmission and emission converging tomography. IEEE Trans Nucl Sci. 1992;39(4):1134–43.

32. Kheruka SC, et al. A new method to correct the attenuation map in simultaneous transmission/emission tomography using 153Gd/67 Ga radioisotopes. J Med Phys Assoc Med Phys India. 2012;37(1):46.

33. Kojima A, et al. Attenuation correction using asymmetric fan-beam transmission CT on two-head SPECT system. Ann Nucl Med. 2004;18(4):315.

34. Lang TF, et al. Description of a prototype emission transmission computed tomography imaging system. J Nucl Med. 1992;33(10):1881–7.

35. Bocher M, et al. Gamma camera-mounted anatomical X-ray tomography: technology, system characteristics and first images. Eur J Nucl Med. 2000;27(6):619–27.

36. Huang B, Law MW-M, Khong P-L. Whole-body PET/CT scanning: estimation of radiation dose and cancer risk. Radiology. 2009;251(1):166–74.

37. Salvatori M, Lucignani G. Radiation exposure, protection and risk from nuclear medicine procedures. Eur J Nucl Med Mol Imaging. 2010;37(6):1225–31.

38. Brenner DJ, Hall EJ. Computed tomography—an increasing source of radiation exposure. N Engl J Med. 2007;357(22):2277–84.

39. Goetze S, et al. Attenuation correction in myocardial perfusion SPECT/CT: effects of misregistration and value of reregistration. J Nucl Med. 2007;48(7):1090–5.

40. Takahashi Y, et al., Attenuation correction of myocardial SPECT images with X-ray CT: effects of registration errors between X-ray CT and SPECT. Ann Nucl Med. 2002; 16(6):431–435.

41. Patton JA, Turkington TG. SPECT/CT physical principles and attenuation correction. J Nucl Med Technol. 2008;36(1):1–10.

42. Kinahan PE, Hasegawa BH, Beyer T. X-ray-based attenuation correction for positron emission tomography/computed tomography scanners. Semin Nucl Med. 2003;33(3):166–79.

43. Kinahan P, et al., Attenuation correction for a combined 3D PET/CT scanner. Med Phys. 1998; 25(10):2046–2053.

44. Seo Y, Wong KH, Hasegawa BH. Calculation and validation of the use of effective attenuation coefficient for attenuation correction in In-111 SPECT. Med Phys. 2005;32(12):3628–35.

45. Seo Y, et al. Correction of photon attenuation and collimator response for a body-contouring SPECT/CT imaging system. J Nucl Med. 2005;46(5):868–77.

46. Berger M. XCOM: photon cross sections database. 2010. http://www.nist.gov/pml/data/xcom/index.cfm

47. Hansen CL, Siegel JA. Attenuation correction of thallium SPECT using differential attenuation of thallium photons. J Nucl Med. 1992;33(8):1574–7.

48. Shibutani T, et al., Characteristics of single-and dual-photopeak energy window acquisitions with thallium-201 IQ-SPECT/CT system. Ann Nucl Med. 2017. 31(7):529–535.

49. Brown JK, et al. Intrinsic dual-energy processing of myocardial perfusion images. J Nucl Med. 2000;41(7):1287–97.

50. Kaplan MS, Haynor DR. Differential attenuation method for simultaneous estimation of activity and attenuation in multiemission single photon emission computed tomography. Med Phys. 1999;26(11):2333–40.

51. Licho R, et al. Attenuation compensation in (99 m Tc) SPECT brain imaging: a comparison of the use of attenuation maps derived from transmission versus emission data in normal scans. J Nucl Med. 1999;40(3):456.

52. Madsen MT, et al. An emission based technique for obtaining attenuation correction data for myocardial spect studies. J Nucl Med. 1993;34(5):P188–8.

53. Krol A, et al. Physical phantom evaluation of EM-IntraSPECT (EMIS) algorithm for non-uniform attenuation correction in cardiac imaging. In: Sonka M, Hanson KM, edtors. Medical Imaging: 2001: image processing, pts 1–3. San Diego, CA, United States; 2001. pp. 934–8.

54. Krol A, et al. EM-IntraSPECT algorithm with ordered subsets (OSEMIS) for non-uniform attenuation correction in cardiac imaging. In: Sonka M, Fitzpatrick JM, editors.Medical Imaging 2002: image processing, vol 1–3. San Diego, CA, United States; 2002. pp. 1022–7.

55. Yamauchi Y, et al. Novel attenuation correction of SPECT images using scatter photopeak window data for the detection of coronary artery disease. J Nucl Cardiol. 2014;21(1):109–17.

56. Okuda K, et al. Attenuation correction of myocardial SPECT by scatter-photopeak window method in normal subjects. Ann Nucl Med. 2009;23(5):501–6.

57. Natterer F. Computerized tomography with unknown sources. SIAM J Appl Math. 1983;43(5):1201–12.

58. Salomon A, Goedicke A, Aach T. Attenuation corrected cardiac SPECT imaging using simultaneous reconstruction and a priori information. IEEE Trans Nucl Sci. 2011;58(2):527–36.

⚡ Springer